

El Niño as a predictor of round sardinella distribution along the northwest African coast

Jorge López-Parages^{a,b,f,*}, Pierre-Amaël Auger^{c,d}, Belén
Rodríguez-Fonseca^a, Noel Keenlyside^e, Carlo Gaetan^b, Angelo Rubino^b,
Maeregu W. Arisido^b, Timothée Brochier^g

^a*Dpto de Física de la Tierra y Astrofísica, UCM-IGEO, Complutense University of
Madrid, Spain*

^b*Dpto di Scienze Ambientali, Informatica e Statistica, Ca Foscari University of Venice,
Italy*

^c*Instituto Milenio de Oceanografía and Pontificia Universidad Católica de Valparaíso,
Valparaíso, Chile*

^d*Laboratoire d'Océanographie Physique et Spatiale (LOPS), IUEM, Brest Universit,
CNRS, IRD, Ifremer, Brest, France*

^e*Bjerknes Centre for Climate Research, Univ. of Bergen, Norway*

^f*CERFACS/CNRS, Climate Modelling and Global Change Team, 42 avenue Gaspard
Coriolis, 31057 Toulouse, France*

^g*Institut de Recherche pour le Développement (IRD), UMMISCO, Sorbonne Universit,
Univertis Cheikh Anta Diop, Dakar, Senegal*

Abstract

The El Niño Southern Oscillation (ENSO) produces global marine environment conditions that can cause changes in abundance and distribution of distant fish populations worldwide. Understanding mechanisms acting locally on fish population dynamics is crucial to develop forecast skill useful for fisheries management. The present work addresses the role played by ENSO on the round sardinella population biomass and distribution in the central-southern portion of the Canary Current Upwelling System (CCUS). A combined physical-biogeochemical framework is used to understand the climate influence on the hydrodynamical conditions in the study area. Then, an evolutionary individual-based model is used to simulate the round sardinella spatio-temporal biomass variability. According to model experiments, anomalous oceanographic conditions forced by El Niño along the African

*Corresponding author

Email address: jlopez@cerfacs.fr (Jorge López-Parages)

1
2
3
4
5
6
7
8
9 coast cause anomalies in the latitudinal migration pattern of the species. A
10 robust anomalous increase and decrease of the simulated round sardinella
11 biomass is identified in winter off the Cape Blanc and the Saharan coast
12 region, respectively, in response to El Niño variations. The resultant anomalous
13 pattern is an alteration of the normal migration between the Saharan
14 and the Mauritanian waters. It is primarily explained by the modulating
15 role that El Niño exerts on the currents off Cape Blanc, modifying therefore
16 the normal migration of round sardinella in the search of acceptable temper-
17 ature conditions. This climate signature can be potentially predicted up to
18 six months in advance based on El Niño conditions in the Pacific.

19
20
21
22 *Keywords:* El Nino, Sardinella aurita, Coastal upwelling, Dynamical
23 oceanography, Atmospheric sciences
24
25

26 27 **1. Introduction**

28 29 *1.1. The round sardinella in the CCUS*

30 Small pelagic fishes populations in the so-called *Eastern Boundary Up-*
31 *welling Systems (EBUS)* are particularly sensitive to global climate change
32 and variability (Bakun, 1990, Bakun et al., 2015, Brochier et al., 2013). These
33 systems, moreover, are of special biological and social importance (Fréon
34 et al., 2009), as they jointly contribute to more than 20% of global fish
35 catches and more than 7% of global marine primary production although
36 they only cover approximately 1% of the total ocean surface (Pauly and
37 Christensen, 1995). The socio-economic relevance of fisheries is especially
38 clear for the Canary Current Upwelling System (CCUS) because of its im-
39 pact on the economies of the northwest African countries (Failler, 2014). This
40 is particularly true in the case of small pelagic fisheries, as they are the main
41 pelagic fisheries in this region in terms of commercial landings (~ 450.000
42 tons per year; Braham et al., 2014).
43
44
45
46
47

48 The CCUS is characterized by a marked spatial and seasonal variability
49 (Chavez and Messié, 2009), especially south of Cape Blanc ($\sim 20^\circ\text{N}$; Carr and
50 Kearns, 2003) and north of the Canary Islands ($\sim 27^\circ\text{N}$; Messié and Chavez,
51 2015), which is associated with the latitudinal migration of the Intertropi-
52 cal Convergence Zone and the accompanying evolution of the Azores high
53 (Wooster et al., 1976). This variability seems to affect the spatial distribu-
54 tion of migratory fish species such as *Sardinella aurita* (Valenciennes, 1847),
55
56
57
58

1
2
3
4
5
6
7
8
9
24 which is the most abundant small pelagic fish in the Senegalese-Mauritanian
10 region. This species, usually called round sardinella, undertakes large north-
11 south migrations over the continental shelf along northwest Africa, with the
12 area of maximum abundance being located approximately between 11°N and
13 25°N (Boëly et al., 1978). Data on fishing effort, fish length distribution, and
14 coastal environmental variability have facilitated recent refinement of scien-
15 tific understating concerning the details of this migration pattern (Braham
16 et al., 2014, Corten et al., 2012, 2017). Recently Brochier et al. (2018) sug-
17 gested that the migration results from 1) an interplay between sea tempera-
18 ture and food availability conditions which both influence the habitat quality
19 of round sardinella, and 2) the effect that coastal currents exert on the pas-
20 sive advection component of round sardinella horizontal movements. These
21 environmental variables (sea temperature, food availability, and currents)
22 also exhibit clear year-to-year differences that modify the seasonal cycle of
23 the CCUS (Benazzouz et al., 2014). However, the mechanisms behind this
24 interannual variability are not well understood. Disentangling the climate
25 influences on the alongshore variability of sea temperature, food abundance,
26 and coastal currents in northwest Africa would shed light on the related re-
27 sponse of the round sardinella population. This understanding is crucial to
28 the development of useful prediction tools for the cooperative management
29 of fish stocks that span political boundaries, and is thus of great importance
30 to the economy and food security of the countries in this region (Failler, 2014).
31
32
33
34
35
36
37
38
39
40

47 *1.2. Global climate as a forcing of round sardinella in the CCUS*

48 Coastal upwelling involves the offshore transport of surface water and
49 its replacement by deep, cold and nutrient-rich waters via Ekman dynam-
50 ics. This is, therefore, a wind-driven process modulated by the intensity of
51 the alongshore winds (Barton et al., 1998). Thus, the interannual variability
52 of surface winds blowing southward alters coastal upwelling, which in turn
53 triggers changes in the ocean mixed-layer temperature, primary productivity,
54 and currents. Thermodynamic processes forced by the surface winds can also
55 alter the upper ocean through heat flux exchanges. Both of the aforemen-
56 tioned mechanisms (dynamical upwelling and thermodynamic heat fluxes)
57 are therefore related to the variability of the surface winds (Polo et al., 2005)
58 and have the potential to alter the round sardinella distribution. Thus, the
59 round sardinella population size and distribution off northwest Africa could
60 be related to large-scale patterns of climate variability due to their impact
61
62
63
64
65

1
2
3
4
5
6
7
8
9
61 on the trade winds blowing in this region (Binet, 1988).
62

63 Understanding the remote responses of fish populations to climate vari-
64 ations is a long standing concern of major importance and broad scientific
65 interest (Overland et al., 2010, Báez et al., 2019). In the case of the CCUS,
66 this issue has been explored in the past, and the results seem to depend on
67 several factors including the chosen methodology. An example of this is the
68 relation with the North Atlantic Oscillation (NAO) which is the dominant at-
69 mospheric variability mode over the North Atlantic in boreal winter (Czaja
70 et al., 2002, Visbeck et al., 2003). The occurrence of upwelling-favorable
71 winds along the northwest African coast is strongly related to the location
72 and strength of the North Atlantic subtropical high (the Azores high) and
73 hence, to the NAO (Meiners et al., 2010). However, recent studies in the
74 CCUS suggest a significant correlation between the NAO and the coastal
75 upwelling intensity when this is derived from the wind stress, but not when
76 this is constructed from the difference in sea surface temperature (hereinafter
77 SST) between the coast and the open ocean (Benazzouz et al., 2014, Crop-
78 per et al., 2014, Narayan et al., 2010). The El Niño-Southern Oscillation
79 (ENSO) phenomenon, which is the dominant pattern of global climate vari-
80 ability at interannual timescales, also impacts the tropical North Atlantic
81 (TNA) through a variety of mechanisms (Giannini et al., 2001, Wang, 2004,
82 Lee et al., 2008, García-Serrano et al., 2017). However, few works have an-
83 alyzed the impact of ENSO on the CCUS and, as in the case of NAO, they
84 conflict on whether a significant signature exists (see e.g., Roy and Reason,
85 2001 and Oettli et al., 2016). Estimating the local signature of these global
86 climate modes on round sardinella population in the CCUS is a priori even
87 harder, as the available abundance data, even with state of the art obser-
88 vational capabilities, are scarce or of low quality. There are also intrinsic
89 limitations in round sardinella catch data associated with the difficulty of
90 distinguishing environmental influences (i.e., not directly related to changes
91 in human activities) and human-related influences. The second includes vari-
92 ability of the market demand, changes in fishing gear and fleet composition,
93 and improvements in fishermen technical skill over time (see e.g., discussion
94 in Bez and Braham, 2014). The recent and interesting observational analy-
95 ses of the CCUS (see e.g., Braham et al., 2014) do not clarify the multiple
96 environmental factors impacting round sardinella spatio-temporal variability.
97

98 New approaches are required to move beyond these conflicting results.

1
2
3
4
5
6
7
8
9
100 Despite their deficiencies, models provide a means to overcome the inherent
101 limitations of observational analysis. For example, investigation of model
102 simulations permit researchers to isolate the climate-related responses from
103 the direct human influence. In the present study, a modeling approach has
104 been used to investigate the influence of ENSO on the interannual variability
105 in the biomass and spatial distribution of a simulated round sardinella
population in the central-southern portion of the CCUS.

106 **2. Material and methods**

107 *2.1. Modeling strategy*

108 The study region (hereinafter referred as CCUS; see Fig. 1) is the upper
109 ocean east of 24°W and between 10°N and 35°N. This geographic area is
110 divided in three distinct regions according to the intensity and seasonal variability
111 of upwelling-favorable winds: the Mauritania-Senegalese zone where
112 the upwelling is seasonal (12°N-19°N), the zone off the Saharan bank (21°N-
113 26°N), and the north Moroccan coast (26°N-35°N), the last two being characterized
114 by year-round upwelling-favorable winds but with different intensities
115 (Benazzouz et al., 2014).

116
117 In this study, a recently developed bio-climatic modeling strategy has
118 been applied. This model approach has been proven as an efficient tool for
119 describing realistic responses of primary productivity and round sardinella
120 to the environment (Auger et al., 2016, Brochier et al., 2018). A scheme
121 of the modeling strategy applied in this study is shown in Fig. 2. Two
122 different parts are identified. In a first step, a hindcast simulation from a
123 coupled hydrodynamic/biogeochemical model produces a realistic 3-D simulation
124 of variability in the fish environment in the CCUS over the period
125 1980-2009. The hydrodynamic environment is simulated by the Regional
126 Oceanic Modeling System ROMS (Shchepetkin and McWilliams, 2005) with
127 an ~ 8 -km resolution and 32 vertical sigma-levels for the CCUS, while the
128 biogeochemical environment is simulated by the PISCES model (Pelagic Interaction
129 Scheme for Carbon and Ecosystem Studies; see Aumont et al.,
130 2003 and Aumont and Bopp, 2006) which simulates phytoplankton and zoo-
131 plankton productivity based on the uptake of nutrients dispersed by ROMS
132 currents. In the present work, the ROMS-PISCES coupled model was forced
133 with the CFSR atmospheric reanalysis (Saha et al., 2010) at a 6-h timescale
134 and with $1/3^\circ$ resolution, and the lateral open boundary conditions are from

1
2
3
4
5
6
7
8
9
10
11
12
13
14
15
16
17
18
19
20
21
22
23
24
25
26
27
28
29
30
31
32
33
34
35
36
37
38
39
40
41
42
43
44
45
46
47
48
49
50
51
52
53
54
55
56
57
58
59
60
61
62
63
64
65

135 monthly model outputs from a simulation of the North Atlantic Ocean in
136 which PISCES is forced by the NEMO hydrodynamic model (Nucleus for
137 European Modelling of the Ocean; Madec, 2008). Please see Auger et al.
138 (2015) for a description of the ROMS-PISCES model configuration, the forc-
139 ing datasets, and the validation of model results using satellite data observa-
140 tions. In a second step, the evolutionary individual-based model *Evol-DEB*
141 (<https://github.com/tbrochier/EvolDEB>) was forced by physical and bio-
142 geochemical outputs from ROMS-PISCES. *Evol-DEB* is an individual-based
143 model that has been proven as an efficient tool to characterize the effect
144 of climate on round sardinella population variables, accounting for environ-
145 mental (e.g., currents, temperature and primary/secondary production) and
146 biological (e.g., fish growth, mortality) factors. The performance of *Evol-*
147 *DEB* has been assessed in the study area through a variety of comparisons
148 including: 1) CPUE (Catch Per Unit Effort) indices calculated from local
149 fisheries monitoring in Senegal and Mauritania, 2) observations of round
150 sardinella body-length distribution from artisanal and industrial fisheries,
151 scientific sampling, and oceanographic research vessels, 3) acoustic observa-
152 tions from oceanographic research vessels, and finally 4) qualitative ecological
153 knowledge from Senegalese fishermen. Brochier et al. (2018) provide a full
154 description of *Evol-DEB* and the validation procedure. The three main envi-
155 ronmental factors influencing the round sardinella dynamics that were tested
156 in the *Evol-DEB* simulations and investigated in the current study were: 1)
157 the currents, 2) the temperature, and 3) the food distribution (from a proxy
158 based on the concentration of plankton in PISCES), each of them averaged
159 over the ocean mixed layer. As described in Brochier et al. (2018), the tem-
160 perature and food proxy were combined to define the *Habitat Quality Index*
161 (*HQI*). In the *Evol-DEB* framework, each aggregation of round sardinella or
162 *super-individuals* is affected by the *HQI* in such a way that the maximization
163 of this *HQI* according to the environmental conditions determines the chance
164 of survival of each super-individual. Round sardinella dynamics also depend
165 on specific round sardinella parameters such as: 1) the swimming capacity, 2)
166 the growth rate, 3) the functional response to the food, and 4) the preferred
167 temperature. Please see Brochier et al. (2018) for details.

168
169 In the present study, the *Evol-DEB* configuration that most realistically
170 captures the response of round sardinella to the environment among all those
171 tested in Brochier et al. (2018) was used: that in which adult populations
172 are sensitive to the currents, and to the temperature and food distributions,

1
2
3
4
5
6
7
8
9
10 173 with maximum swimming speed of 4.5 body-length per second, and with
11 174 the preferred temperature determined by the corresponding natal temper-
12 175 ature. Each *Evol-DEB* simulation lasted for 30 years, from 1980 to 2009,
13 176 with a seeding procedure taking place in 1980. The 1980-1984 period was
14 177 viewed as a spin-up period, considering that the maximum longevity of super-
15 178 individuals is ~ 4.5 years. The choice of the initialization of environmental
16 179 conditions was shown to have little effect on the subsequent emerging inter-
17 180 annual variability, resulting therefore in an effective output period of 25 years
18 181 (from 1985 to 2009). Please note that although the environmental forcings
19 182 which influence round sardinella variability in *Evol-DEB* are the ocean vari-
20 183 ables provided by *ROMS-PISCES*, the atmospheric forcing from the CFSR
21 184 reanalysis used to run the *ROMS-PISCES* model do contain information of
22 185 any potential teleconnection between the global climate and the local round
23 186 sardinella population biomass. Therefore, the described comprehensive mod-
24 187 eling framework (*ROMS-PISCES* and *Evol-DEB*) will capture a significant
25 188 response to global climate forcing, depending on the forcing persistence and
26 189 the noise generated internally by the models. If any climate-round sardinella
27 190 teleconnection is identified in the analysis of final model outputs (Fig. 2),
28 191 it must have entered into the model setup through the applied boundary
29 192 conditions, and it should be strong enough to be passed among the physical-
30 193 biogeochemical-ecosystem components of the models involved.
31
32
33
34
35
36
37

38 195 *2.2. Exploring the relation with the global climate*

39
40 196 The aim of this study was to understand how the latitudinal distribu-
41 197 tion of simulated adult round sardinella biomass over the northwest African
42 198 continental shelf is altered by changes in the local environmental conditions
43 199 and to explore the possible role played by remote climate forcings. The
44 200 biomass over the continental shelf captures most of the north-south round
45 201 sardinella variability, as the stocks are generally tied to the coastal areas
46 202 where the highest food production occurs. This feature is well represented
47 203 by the *ROMS-PISCES-Evol-DEB* model framework (Figs. 3a-b). Based
48 204 on the latter, various latitude vs months Hovmöller diagrams were plotted
49 205 for different fields by averaging the corresponding variable across longitudes
50 206 (Figs. 3c-f). To reduce the degrees of freedom and to efficiently characterize
51 207 round sardinella variability, Empirical Orthogonal Function (EOF; Lorenz,
52 208 1956) analysis was performed on the yearly Hovmöllers of modeled round sar-
53 209 dinella biomass (anomalous round sardinella biomass averaged in longitude
54
55
56
57
58
59
60
61
62
63
64
65

1
2
3
4
5
6
7
8
9
10
11
12
13
14
15
16
17
18
19
20
21
22
23
24
25
26
27
28
29
30
31
32
33
34
35
36
37
38
39
40
41
42
43
44
45
46
47
48
49
50
51
52
53
54
55
56
57
58
59
60
61
62
63
64
65

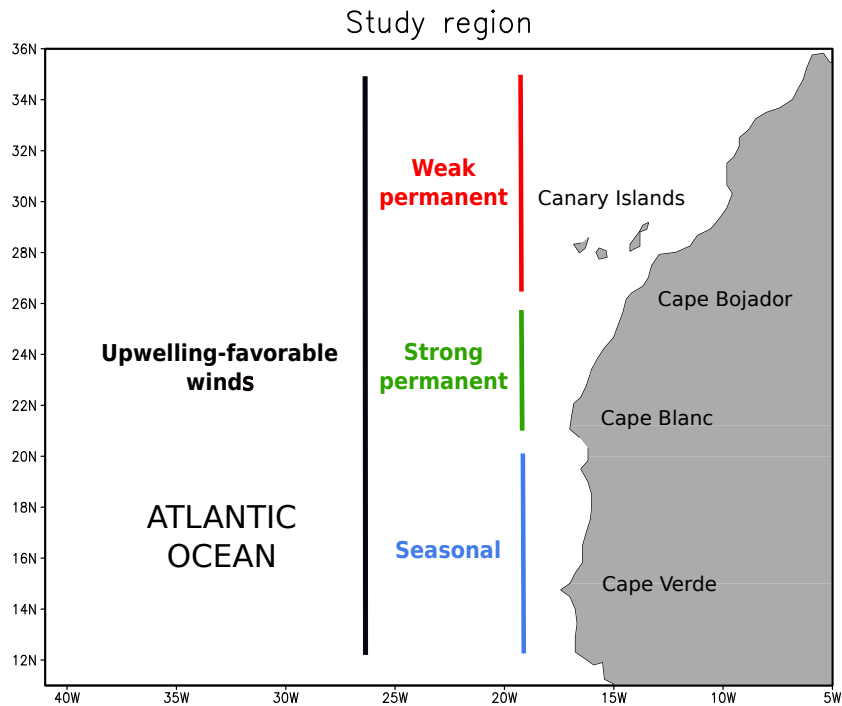


Figure 1: Study region and upwelling zones inside it. This figure is only used for illustrative purposes.

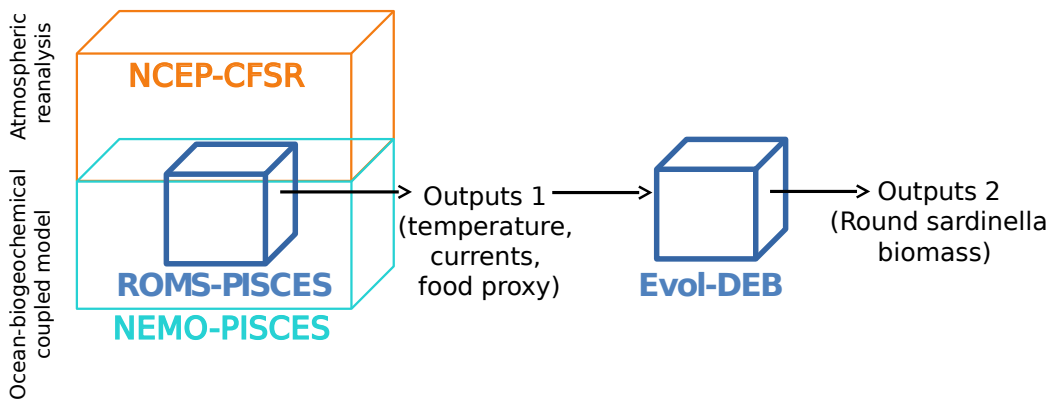


Figure 2: Modeling framework. The abbreviations used are: National Centers for Environmental Prediction (NCEP), Climate Forecast System Reanalysis (CFSR), Regional Oceanic Modeling System (ROMS), Pelagic Interaction Scheme for Carbon and Ecosystem Studies (PISCES), Nucleus for European Modelling of the Ocean (NEMO), and evolutionary individual-based model with dynamic energy budget (Evol-DEB)

1
2
3
4
5
6
7
8
9
10
11
12
13
14
15
16
17
18
19
20
21
22
23
24
25
26
27
28
29
30
31
32
33
34
35
36
37
38
39
40
41
42
43
44
45
46
47
48
49
50
51
52
53
54
55
56
57
58
59
60
61
62
63
64
65

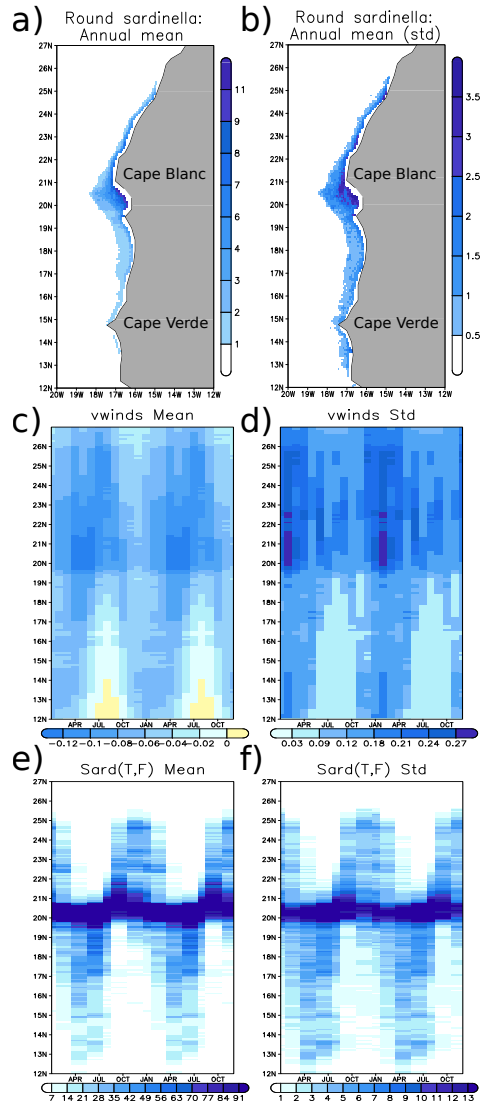


Figure 3: **Annual mean and seasonal cycles from the modeling framework.** In top panels the annual mean of round sardinella biomass (panel a), and the interannual variability of round sardinella biomass (in terms of standard deviation; panel b), from *Evol-DEB*. Units in tons/m². Central panels: Seasonal cycles (mean in panel c, negative southward, and variability, in terms of standard deviation, in panel d) of the meridional component of the wind stress (from *ROMS-PISCES*; units in N/m²). Bottom panels: as panels c and d but for the simulated round sardinella biomass (from *Evol-DEB*; units in tons/m²). In the case of the meridional wind stress, the fields are averaged from the coast to the isobath 1000 meters.

210 along the northwest African coast). The associated standardized principal
 211 components (PC) show the time evolution of the scores of the EOFs, thus
 212 identifying the years in which these EOFs are manifest. The link between
 213 these EOFs (or round sardinella modes) and the climate was evaluated in
 214 terms of regression and composites maps. To analyze the link with the large-
 215 scale environment (i.e., global climate), SST data from HadISST1 (Rayner
 216 et al., 2003), and global observed sea level pressure data (SLP) and surface
 217 winds from the NCEP Climate Forecast System Reanalysis (CFSR; Saha
 218 et al., 2010) were used. The HadISST dataset was also used to calculate
 219 the Niño 3.4 index (SST averages over the area 170-120°W, 5°S-5°N), and
 220 the CFSR reanalysis was chosen to be consistent with the atmospheric condi-
 221 tions prescribed in the *ROMS-PISCES* simulation. Sea temperature and
 222 ocean currents averaged over the top 50 m of the water column (from *ROMS-*
 223 *PISCES*) were used to characterize the local environmental variability (i.e.,
 224 local climate). Please see the Table 1 for a summary of the data used in
 225 the present study. The statistical significance was assessed by a bootstrap
 226 re-sampling procedure with replacement. At the end of the study, a lead-lag
 227 correlation analysis has been applied for exploring the predictive potential
 228 of round sardinella distribution in the CCUS from equatorial Pacific SSTs.
 229 In that case, the non-parametric test described by Ebisuzaki (1997), and
 230 specially designed to avoid serial correlation, was used.

Table 1: Summary of the data used in the present study.

| Variable | Source | Reference |
|--------------------------|--------------------|------------------------|
| (Global) SST | HadISST | Rayner et al. (2003) |
| (Global) SLP | CFSR | Saha et al. (2010) |
| (Global) Surface winds | CFSR | Saha et al. (2010) |
| Sea temperature | <i>ROMS-PISCES</i> | Auger et al. (2015) |
| Ocean currents | <i>ROMS-PISCES</i> | Auger et al. (2015) |
| Wind stress | <i>ROMS-PISCES</i> | Auger et al. (2015) |
| Round sardinella biomass | <i>Evol-DEB</i> | Brochier et al. (2018) |

231 A linear regression prediction model was also constructed in the present
 232 study to illustrate the potential of the results obtained for skillful prediction.
 233 This prediction model is based on the “leave one out” method (Wilks, 2011),

1
2
3
4
5
6
7
8
9
234 which produces a forecast for each time t (year) using only data at other
235 times (years) distinct from t .

236 **3. Results**

237 *3.1. Anomalous migration further north of Cape Blanc*

238 The present modeling framework produces a coherent migration pattern
239 of round sardinella population (Fig. 3e): to the south in spring reaching
240 the Senegalese-Mauritanian waters in summer, and to the north in autumn,
241 reaching the Saharan waters in winter (Corten et al., 2012). This migra-
242 tion pattern from *Evol-DEB* is associated with the atmospheric conditions
243 imposed on *ROMS-PISCES*. Evidence from that fact is the consistency be-
244 tween the meridional wind stress (V_{st} , negative southward; see Fig. 3c) and
245 the round sardinella biomass further north of Cape Blanc ($\sim 21^\circ\text{N}$), a region
246 characterized by strong alongshore currents to the south, in the so-called
247 *Cape Blanc Transition Zone*. Only in early winter, when the southward
248 wind stress in this area weakens (Fig. 3c), a certain percentage of round
249 sardinella (those with the strongest swimming capacity) reach the Saharan
250 waters (Fig. 3e), where the high food availability contributes to relatively
251 high HQI all year round (Brochier et al., 2018). Interestingly, this minimum
252 of southward wind stress in winter coincides with the strongest variability
253 of this variable off Cape Blanc (Fig. 3d) and, with increased variance in
254 round sardinella biomass north of that cape (Fig. 3f). The variability is
255 expressed here in terms of the standard deviation, representing the degree
256 of deviation of each variable with respect to its corresponding seasonal cycles.

257
258 Hence, Fig. 3 points to the existence of year-to-year variability fur-
259 ther north of Cape Blanc in both the environment and the round sardinella
260 biomass. To assess the correlation between these variabilities, an EOF anal-
261 ysis was performed on the yearly Hovmöllers of round sardinella biomass
262 anomaly along the coast, from 19°N to 26°N , and for the January to March
263 season. This season was selected in order to cover those months with the
264 maximum variability in the alongshore wind stress (V_{st} ; Fig. 3d). The Prin-
265 cipal Component (hereinafter PC1) of the leading EOF mode, which explain
266 46% of the total variance, was then lag-regressed on the yearly Hovmöllers
267 of round sardinella biomass (plotted from the previous July to the follow-
268 ing June for a better comparison with the seasonal cycles; see Fig. 4a). A

1
2
3
4
5
6
7
8
9
10
11
12
13
14
15
16
17
18
19
20
21
22
23
24
25
26
27
28
29
30
31
32
33
34
35
36
37
38
39
40
41
42
43
44
45
46
47
48
49
50
51
52
53
54
55
56
57
58
59
60
61
62
63
64
65

269 dipole structure, with negative anomalies off the Saharan coast and posi-
270 tive anomalies off Cape Blanc was obtained from early to late winter. This
271 analysis indicates that anomalous meridional migration of round sardinella
272 may play a key role in determining the biomass and distribution of round
273 sardinella along the northwest African coast.

274 275 *3.2. Role played by the environment*

276 Firstly, the role of the environment in stimulating this leading mode of
277 variability was investigated by analyzing an additional *Evol-DEB* simulation
278 with climatological forcings obtained by averaging the ROMS-PISCES out-
279 puts for the entire period (1980-2009). That is, instead of forcing *Evol-DEB*
280 with the varying environmental conditions from 1980 to 2009 (*Inter experi-*
281 *ment* in Table 2), it was forced with the climatological averaged conditions
282 in that period (*Control experiment* in Table 2). Therefore the interannual
283 variability within the ROMS-PISCES outputs was removed such that this
284 simulation may be interpreted as a control simulation for *Evol-DEB*. EOF
285 analysis shows that the dipolar structure is missing in this control simulation
286 (Fig. 4b), indicating that the response in the *Inter experiment* was forced
287 by the environment.

Table 2: Overview of the set of *Evol-DEB* simulations run for the present study. Round sardinella dependence refers to those environmental parameters (Temperature, Food or both), from ROMS-PISCES, influencing the habitat quality of the species in *Evol-DEB*. Food contribution is quantified through a proxy defined as the sum of the biomass in the four PISCES plankton compartments (please see Brochier et al. 2018 for details).

| Experiment | ROMS-PISCES forcing | round sardinella dependence |
|------------|-----------------------|-----------------------------|
| Inter | 1980 – 2009 | T,F |
| Control | $(1980 - 2009)_{avg}$ | T,F |
| Inter T | 1980 – 2009 | T |
| Inter F | 1980 – 2009 | F |

288 289 *3.3. El Niño emerges as a potential forcing*

290 Considering the important role of SSTs in the global climate teleconnec-
291 tions, next the PC1 from the *Inter experiment* was regressed on the global

Table 3: Linear correlations among the distinct PC1 obtained in the set of simulations recapitulated in Table 2.

| Correlation | PC1(Control) | PC1(Inter T) | PC1(Inter F) |
|-------------|--------------|--------------|--------------|
| PC1(Inter) | 0.02 | 0.88 | 0.41 |

SSTs of the same season. A noticeably clear and significant ENSO pattern emerged in the tropical Pacific (Fig. 5a). The same ENSO structure appeared when just an index based on the averaged accumulation of round sardinella off Cape Blanc was projected onto the SSTs (not shown). The question emerging therefore is whether this anomalous response of round sardinella in northwest Africa (the aforementioned dipolar structure) is caused by ENSO or if it is a statistical artifact.

Before exploring the dynamical mechanisms linking ENSO and round sardinella spatio-temporal variability, the environmental response to ENSO in northwest Africa that causes the anomalous distribution of modeled round sardinella biomass along the coast was investigated. To address this question, recall that both temperature and food distribution influence the HQI in the previously described *Evol-DEB* simulations (*Inter Experiment & Control Experiment*), as these follow the more realistic configuration according to Brochier et al. (2018). Assuming that the sardinella dependence on their habitat quality is based only on the food availability (*Inter F experiment* in Table 2) leads to the disappearance of the previously analyzed dipolar structure (Fig. 6c). However, this is not the case when the HQI is based only on sea temperature (Fig. 6a). Therefore it could be concluded that the dipolar structure identified in Fig. 4a is associated with the round sardinella’s dependence on water temperature as represented in the model. Please note that this does not mean that round sardinella only follows the variability of the water temperature. Others factors, such as alongshore currents, could also play a major role in altering the round sardinella variability. However, this major role would only emerge when round sardinella migrates towards areas with optimal temperature conditions. If this dependence on the temperature is removed, the effect of ENSO on round sardinella also disappears. This effect of temperature on the teleconnection is reinforced by the correlations among the leading principal components of round sardinella’s biomass in the

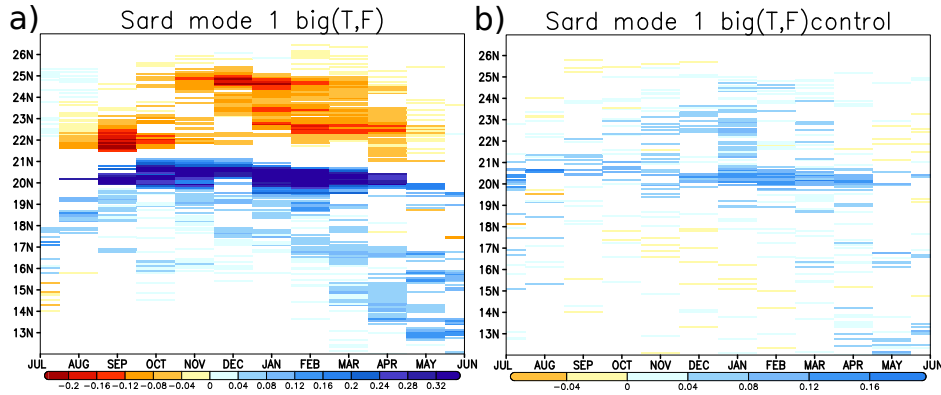


Figure 4: **Round sardinella EOF: a mode forced by the environment.** Leading EOF of the anomalous sardinella biomass (calculated from 19°N to 26°N and for the JFM season; units in tons/m² per std in the PC1) obtained in: a) the Inter experiment and b) the Control experiment. Shading areas represent the 90% significant response according to a bootstrap technique with replacement. Please note that blue and red colors indicate positive and negative anomalies of biomass respectively.

different simulations (see Table 3). Furthermore, the regression maps of the leading PCs on global SSTs showed that the ENSO pattern persists when the round sardinella dependence on food is removed (Inter T experiment; see Fig. 6b), but disappears when the round sardinella dependence on temperature is removed (Inter F experiment; see Fig. 6d).

There is still a remaining aspect to fully characterize the ENSO-round sardinella teleconnection: its linearity in relation to the ENSO phase. In particular, the question emerging is whether the identified ENSO signal is caused by the influence of both warm (El Niño) and cold (La Niña) ENSO phases. Comparing the evolution of the Niño 3.4 index and the standardized round sardinella PC1 (Inter Experiment) revealed that the three highest values of PC1 coincide with three (1988, 1998, 2003) of the four highest values of the Niño 3.4 index. Nevertheless, there is an absence of coincidence in time between the negative values of the Niño 3.4 index and the peaks of the round sardinella PC1. This appears more clearly when comparing the negative composite patterns (those years in which the index is below -1 standard deviation) of SSTs for the Niño 3.4 index and the round sardinella PC1 (Supplementary material; Fig. S1): this indicates that a negative occurrence of the round sardinella mode is more related to the NAO than to the Pacific

1
2
3
4
5
6
7
8
9
10
11
12
13
14
15
16
17
18
19
20
21
22
23
24
25
26
27
28
29
30
31
32
33
34
35
36
37
38
39
40
41
42
43
44
45
46
47
48
49
50
51
52
53
54
55
56
57
58
59
60
61
62
63
64
65

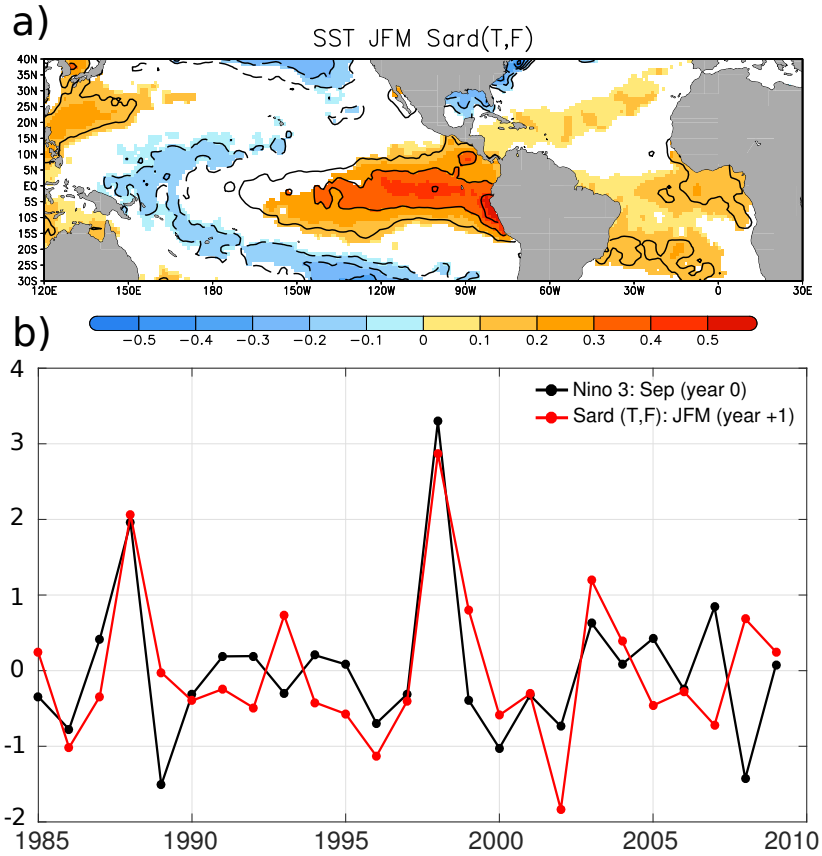


Figure 5: **Round sardinella EOF: a mode forced ENSO.** a) Regression map of the round sardinella mode of biomass on anomalous SSTs (units in degrees per std in the PC1); shading areas represent the 90% significant response according to a bootstrap technique with replacement. b) standardized PC1 of the round sardinella mode (red line) and the standardized Niño 3.4 index in the previous September (black line).

1
2
3
4
5
6
7
8
9
10
11
12
13
14
15
16
17
18
19
20
21
22
23
24
25
26
27
28
29
30
31
32
33
34
35
36
37
38
39
40
41
42
43
44
45
46
47
48
49
50
51
52
53
54
55
56
57
58
59
60
61
62
63
64
65

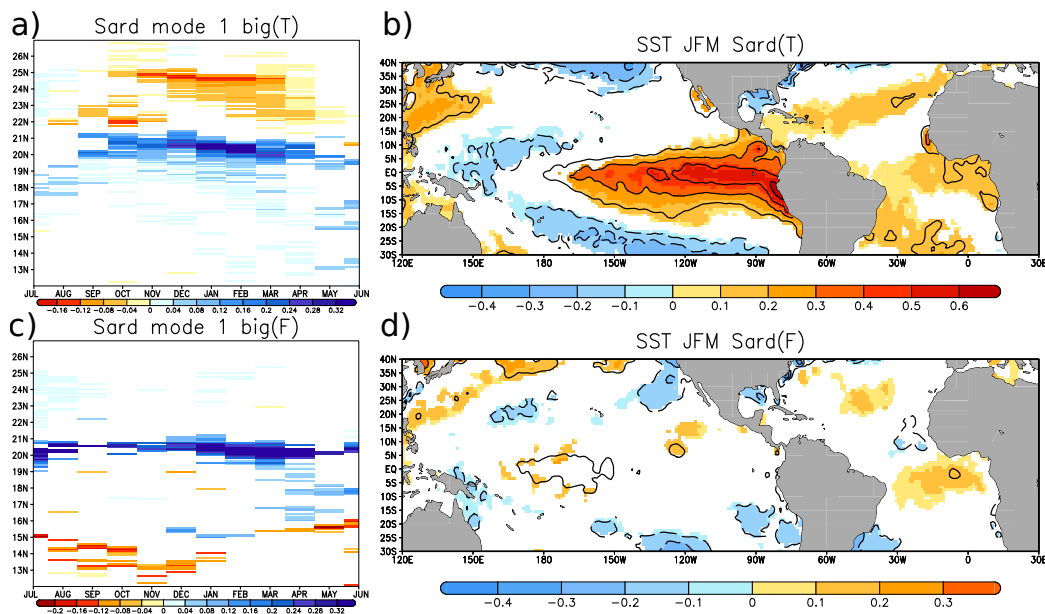


Figure 6: **Round sardinella EOF: a mode highlighting the role of temperature.** a) leading EOF of anomalous sardinella biomass for the Inter T Experiment, b) SST regression for the Inter T Experiment, c) leading EOF of anomalous sardinella biomass for the Inter F Experiment, d) SST regression for the Inter F Experiment. Shading areas represent the 90% significant response according to a bootstrap technique with replacement.

1
2
3
4
5
6
7
8
9
342 SSTs. Thus, the ENSO-round sardinella link found in the described model-
10 ing framework is only triggered by warm ENSO phases (El Niño).
11
12
13

14 345 *3.4. Dynamical mechanisms*

15
16 To address the dynamical explanations supporting this influence of El
17 Niño episodes on the modeled round sardinella biomass, early winter (from
18 November to January) and late winter (from February to March) were sepa-
19 rated based on: 1) the different evolution of El Niño episodes and their related
20 responses in the TNA, and 2) the very different feature of round sardinella
21 migrations along the northwest African coast before and after January. Re-
22 garding the former, the response to ENSO in early winter is characterized by
23 anomalous horizontal and vertical flows in the western TNA (Wang, 2002)
24 and by an East Atlantic (EA) like pattern further north over the North At-
25 lantic (King et al., 2018). From January onwards, an atmospheric Rossby
26 wavetrain forced from the tropical Pacific crosses the North Pacific-American
27 region and reaches the TNA (Enfield and Mayer, 1997). This response, to-
28 gether with the documented ENSO influence on the Walker and Atlantic
29 Hadley circulation cells (Wang, 2004), explains the ENSO-TNA teleconnec-
30 tion in late winter. Regarding the round sardinella migrations along the
31 northwest African coast, remarkable differences are also identified between
32 early and late winter. Before January, round sardinella are normally moving
33 northward to reach the Saharan waters (see Fig. 3e), where there is high food
34 availability resulting in high HQI (Brochier et al., 2018). After January, how-
35 ever, round sardinella begin a southward migration. The underlying reasons
36 include the declining food production when upwelling off Cap Blanc retracts
37 to very coastal waters, and the drop in water temperature to values below the
38 species tolerance. Furthermore, it is worth reminding that a natural instinct
39 of round sardinella to search its natal homing temperature is implemented
40 in Evol-DEB. Thus, as both the upwelling intensity and the water tempera-
41 ture could be altered by the El Niño influence in the study region, a related
42 response in round sardinella is expected.
43
44
45
46
47
48
49
50
51

52 374 *3.4.1. Early-winter*

53
54 In early-winter (Fig. 7a), a marked El Niño pattern is identified in those
55 years in which the anomalous round sardinella mode (Fig. 6a) is manifested.
56 A weakening of the trade winds has been identified in the western TNA, in
57
58
59
60
61
62
63
64
65

1
2
3
4
5
6
7
8
9
10 378 agreement with the documented response to ENSO (Wang, 2002). The resul-
11 379 tant anomalous northward winds turn right at approximately 25-30°N. This
12 380 deflection is explained by the EA-like pattern found over the North Atlantic
13 381 and is consistent with the most recent literature (King et al., 2018). Conse-
14 382 quently, an anomalous increase of the subtropical winds is detected to the east
15 383 that reaches the African continent. For illustrative purposes, the significant
16 384 response of the surface wind (black vectors in Fig. 7a) is calculated with re-
17 385 spect to the zonal component in Nov-Jan. In the ROMS-PISCES simulation,
18 386 this global signal is associated with a significant increase of the zonal wind
19 387 stress to the east (black vectors in Figs. 8a-b) and, even more important for
20 388 this case, with an anomalous increase of the alongshore currents to the south
21 389 (shaded areas in Fig. 8b). Note that this enhancement of the alongshore cur-
22 390 rents is particularly intense off Cape Bojador and Cape Blanc, although it is
23 391 not associated with significant upwelling-favorable wind anomalies. Off Cape
24 392 Blanc, it appears to coincide with the anomalous accumulation of round sar-
25 393 dinella biomass simulated by *Evol-DEB* (Fig. 6a). Thus, the response to El
26 394 Niño drives anomalous southward alongshore currents in early winter, along
27 395 the *Cape Blanc Frontal Zone*, that counters the normal northward migration
28 396 of round sardinella. As a consequence, an anomalous increase (decrease) of
29 397 biomass emerges at $\sim 20\text{-}21^\circ\text{N}$ ($\sim 24\text{-}25^\circ\text{N}$).
30
31
32
33
34
35
36
37

38 399 *3.4.2. Later-winter*

39 400 In late winter, the round sardinella mode is related to northward wind
40 401 anomalies in the eastern part of the TNA that occur after the peak of El Niño
41 402 episodes and which are particularly intense along the northwest African coast
42 403 (the significant signal of the meridional component is highlighted as black
43 404 vectors in Fig. 7b). The weakened Azores high identified in Fig. 7b is in
44 405 agreement with the documented late winter influence of ENSO caused by the
45 406 thermally-driven direct circulation (Wang, 2004) and Rossby wave activity
46 407 (Enfield and Mayer, 1997). The anomalous SST pattern identified here is also
47 408 as expected (Ham et al., 2014). The resultant alongshore winds in northwest
48 409 Africa weakens the upwelling due to a reduction of the Ekman transport and
49 410 hence, an intense and significant anomalous warming is detected along the
50 411 coast. The ROMS-PISCES model reproduces the anomalous warming along
51 412 the coast as a consequence of the attenuated coastal upwelling (Fig. 8c) and
52 413 simulates northward coastal current anomalies (Fig. 8d).
53
54
55
56
57
58
59
60
61
62
63
64
65

1
2
3
4
5
6
7
8
9
10
11
12
13
14
15
16
17
18
19
20
21
22
23
24
25
26
27
28
29
30
31
32
33
34
35
36
37
38
39
40
41
42
43
44
45
46
47
48
49
50
51
52
53
54
55
56
57
58
59
60
61
62
63
64
65

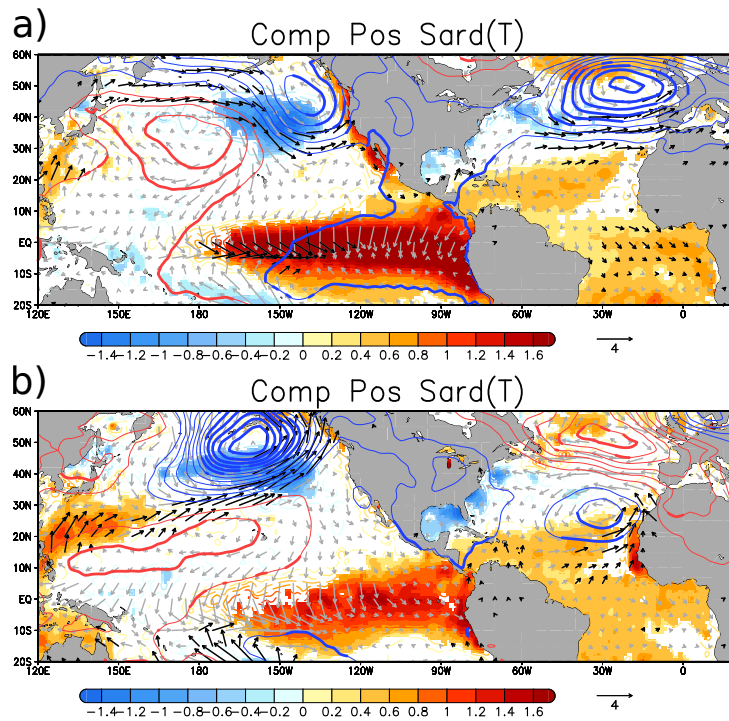


Figure 7: **Global signature of the round sardinella mode.** a) positive composite maps in early winter based on the standardized PC1 of the anomalous sardinella mode (years above 1 standard deviation), b) as in a) but for late winter. In both cases the fields plotted are: anomalous SST (shaded the significant response; units in degrees), anomalous SLP (contoured; thick contoured the significant response), and anomalous surface wind (grey vectors; units in m/s). Significance at the 90% level based on a bootstrap technique with replacement.

1
2
3
4
5
6
7
8
9
10
11
12
13
14
15
16
17
18
19
20
21
22
23
24
25
26
27
28
29
30
31
32
33
34
35
36
37
38
39
40
41
42
43
44
45
46
47
48
49
50
51
52
53
54
55
56
57
58
59
60
61
62
63
64
65

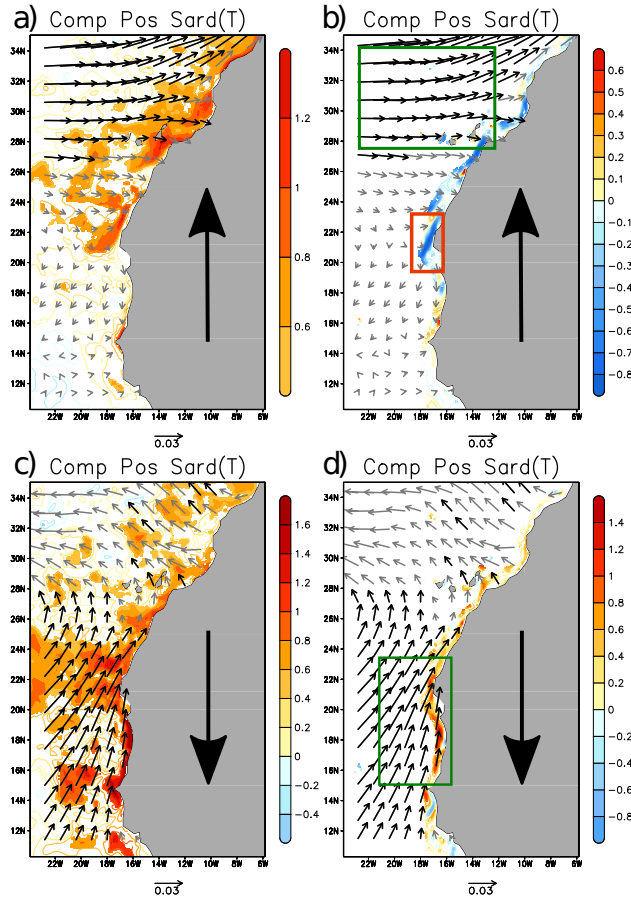


Figure 8: **Local signature of the round sardinella mode (ROMS-PISCES).** Upper panels corresponds to the composites maps in early winter (Nov-Jan) and bottom panels to the composites maps in late winter (Feb-Mar). Left panels show the anomalous temperature in the top 50 meters of the water column (shaded the significant response; units in degrees). In the right panels the anomalous meridional currents of the top 50 meters of the water column (shaded the significant response, units in $10 \times \text{m/s}$). The anomalous wind stress (vectors; units in N/m^2) are shown on all panels. Only the water surfaces with less than 1000 meters depth are plotted due to these waters house the vast majority of round sardinella. The significant response in the zonal (meridional) anomalous wind stress is highlighted for early (late) winter with black vectors. Significance at the 90% level based on a bootstrap technique with replacement. Large pointing-arrows indicate the migration pattern of the species in early and late winter according to the seasonal cycle of biomass.

1
2
3
4
5
6
7
8
9
10
11
12
13
14
15
16
17
18
19
20
21
22
23
24
25
26
27
28
29
30
31
32
33
34
35
36
37
38
39
40
41
42
43
44
45
46
47
48
49
50
51
52
53
54
55
56
57
58
59
60
61
62
63
64
65

415 To understand the round sardinella response, it is important to realize
416 that although the presence of the species has been reported in a very large
417 range of temperatures, from $\sim 10^{\circ}\text{C}$ in the Mediterranean Sea (Tsikliras and
418 Antonopoulou, 2006) up to 29°C in Senegal (Marchal, 1991), the highest
419 biomass in northwest Africa has been detected for a range of SSTs between
420 21°C and 25°C (Diankha et al., 2015). Thus, waters excessively cold (be-
421 low 19°C) or excessively warm (above $26\text{-}27^{\circ}\text{C}$) host low round sardinella
422 biomass. This feature is included in Evol-DEB by a correction factor applied
423 to all the energy fluxes between the model compartments. Thus, one can
424 understand why in late winter, under normal conditions, the drop of water
425 temperatures off the Saharan bank to values below 19°C contributes to a
426 southward migration (favored by the climatological southward currents) of
427 round sardinella.

428
429 In this context, the anomalous warming generated by El Niño in late
430 winter off the African coast (Fig. 8c) increases the absolute temperature of
431 the water column off Cape Blanc to around 20°C , significantly warmer than
432 the normal $\sim 18^{\circ}\text{C}$ there at that time of the year (see also Fig. S2 in Supple-
433 mentary material). This fact, together with the reduced passive advection
434 of round sardinella due to the anomalous weakening of the southward cur-
435 rents south of Cape Blanc during El Niño years (Fig. 8d), explains how the
436 anomalous accumulation of biomass at $20\text{-}21^{\circ}\text{N}$ latitude identified in Evol-
437 Deb in association with the leading EOF mode (Fig. 6a) persists until well
438 into the spring season. However, the persistence of negative biomass anoma-
439 lies further north of Cape Blanc seems to be a reminiscent effect of the fewer
440 individuals who reached the Saharan waters at the beginning of the winter
441 season. The slight positive biomass anomalies detected between 13°N and
442 19°N (Fig. 4a) in late winter might reflect the response of round sardinella
443 to the warmer and more favorable water temperature conditions along the
444 Mauritanian-Senegalese coast as a consequence of the reduced upwelling.

445 446 *3.5. Potential predictability of round sardinella population biomass*

447 One of the main contributions of this work is that it provides the basis for
448 the development of a future seasonal forecasting tool of round sardinella lat-
449 itudinal distribution along northwest Africa based on El Niño-related SSTs,
450 which can be observed from the space. In particular, high lagged correlations
451 between the round sardinella mode in winter (see Fig. 6a) and the Niño 3

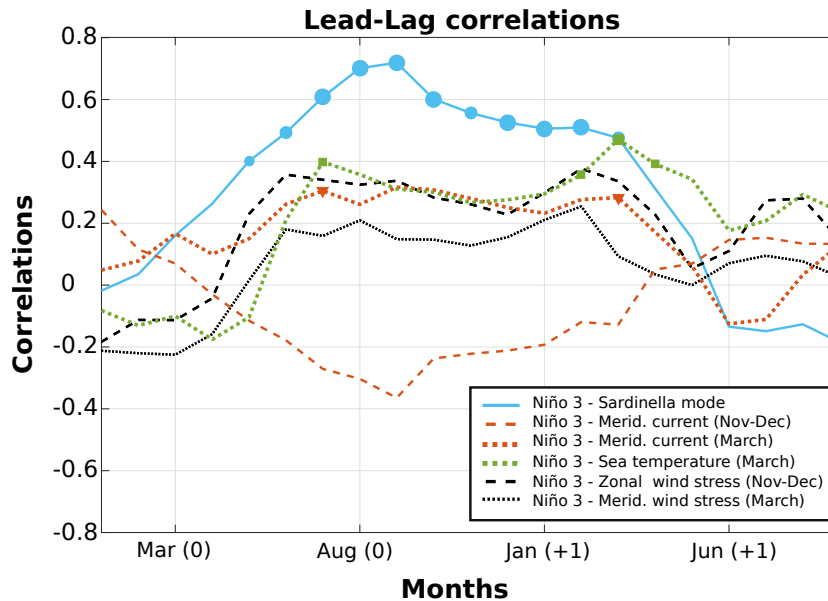


Figure 9: **Lead-lag correlations.** Blue solid line shows the linear correlation between the Niño 3 index at different lags and the leading sardinella mode (i.e., the corresponding PC) in JFM (year +1; see Fig. 6a). The same correlations with the Niño 3 index are shown for: 1) the meridional current (top 50m of the water column) off Cape Blanc in Nov-Dec (dashed brown line) and March (dotted brown line), and 2) the water temperature (top 50m of the water column) off Cape Blanc in March (green dotted line). The region off Cape Blanc is defined as the area within the red square indicated in Fig. 8b. Large, medium and small sized symbols represent correlations at the 99%, 95% and 90% confidence level respectively according to Ebisuzaki (1997). Black dashed (dotted) line shows the correlation between the leading round sardinella mode and the zonal (meridional) wind stress averaged within the green boxes of Fig. 8.

index suggest the potential for skillful prediction (see blue line in Fig. 9). The El Niño-round sardinella link appears stronger with the eastern tropical Pacific than with the central tropical Pacific (Supplementary material; Fig. S3), which is consistent with the available literature related to the ENSO-TNA teleconnection (Taschetto et al., 2016).

A linear regression prediction model based on the “leave one out” method (Wilks, 2011) has been constructed to predict, for the two strongest Eastern El Niño episodes of the simulated period (1987/88 and 1997/98), the anomalous distribution of round sardinella from El Niño 3 SSTs in the previous September. The resultant predictions and the corresponding patterns esti-

1
2
3
4
5
6
7
8
9
10
11
12
13
14
15
16
17
18
19
20
21
22
23
24
25
26
27
28
29
30
31
32
33
34
35
36
37
38
39
40
41
42
43
44
45
46
47
48
49
50
51
52
53
54
55
56
57
58
59
60
61
62
63
64
65

463 mated by *Evol-DEB* are shown in Figure 10. One could reasonably think that
464 our prediction skill, based on the leading EOF of round sardinella biomass in
465 winter, should be almost completely dependent on the information coming
466 from the specific episodes to be predicted, as they correspond to extreme val-
467 ues of the aforementioned EOF. However, if so, the forecast skill assessed with
468 our cross-validation method should be close to zero. As shown in Fig. 10a-d,
469 this is not the case: the anomalous SSTs in the Niño 3 region in Septem-
470 ber (i.e., September 1987 and September 1997, respectively) are enough to
471 predict realistically the anomalous distribution of round sardinella in the
472 following winter and spring along the northwest African coast. Although
473 robust, this predictive skill seems to be only valid for eastern (and partic-
474 ularly strong) El Niño years, as appreciated in the comparison between the
475 modeled and the predicted evolution of round sardinella population biomass
476 in a particular location (Cape Blanc; see bottom panel in Fig. 10e).
477

478 4. Summary and discussions

479 The present study provides, for the first time, a consistent mechanism
480 explaining how a remote climatic phenomenon (El Niño, understood as the
481 ENSO warm phases) is able to alter the latitudinal migration pattern of
482 *Sardinella aurita* (or round sardinella) in the narrow coastal band along
483 northwest Africa. This has been possible through an innovative modeling
484 strategy specifically designed to explore potential environmental drivers of
485 spatio-temporal population variability of this species in the region. This
486 modeling framework has been previously validated in the study region and
487 highlighted the strong effect that the local environment may play on the dis-
488 tribution of round sardinella along this coast (Brochier et al., 2018).
489

490 Modeling results point out that the round sardinella response to El Niño
491 is an anomalous migration pattern of this species during boreal winter be-
492 tween the Mauritanian and the Saharan waters. As a consequence, the model
493 simulates an anomalous increase (decrease) of round sardinella biomass off
494 the Cape Blanc (Saharan coast) during El Niño years. Distinct bio-physical
495 mechanisms take place in early and late winter to sustain this modeled ma-
496 rine ecological response to El Niño (if needed, see scheme in Fig. S4 of
497 Supplementary material). This difference between early and late winter is
498 not really surprising, as 1) the climatological responses to El Niño evolve

1
2
3
4
5
6
7
8
9
10
11
12
13
14
15
16
17
18
19
20
21
22
23
24
25
26
27
28
29
30
31
32
33
34
35
36
37
38
39
40
41
42
43
44
45
46
47
48
49
50
51
52
53
54
55
56
57
58
59
60
61
62
63
64
65

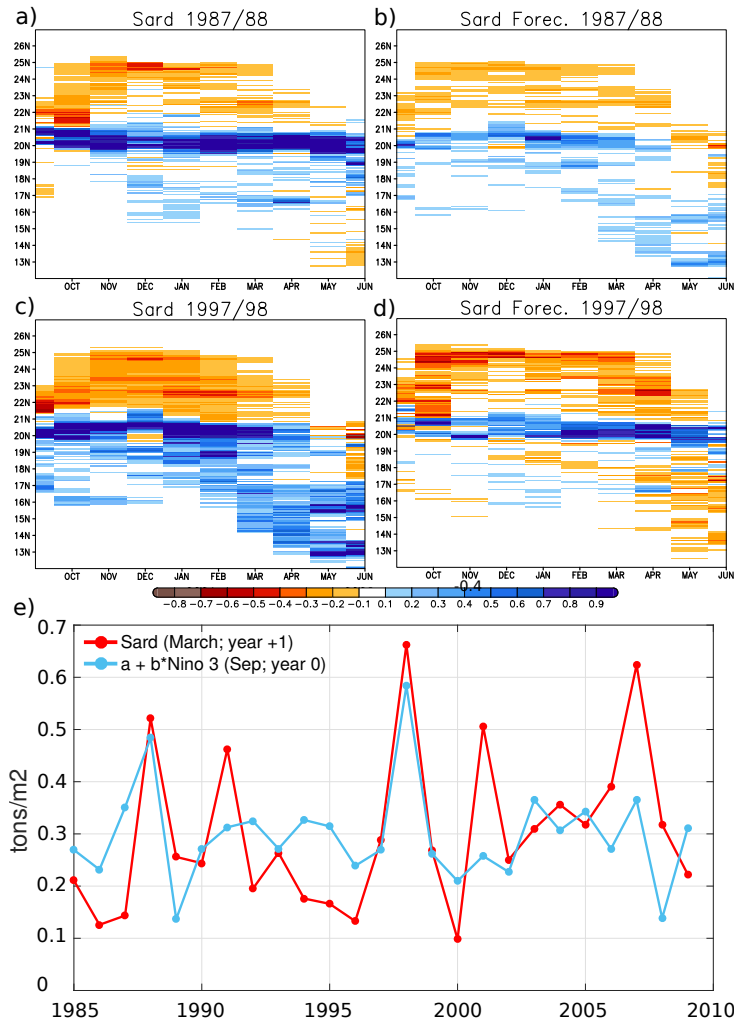


Figure 10: **Potential predictability.** Round sardinella biomass anomaly from *Evol-DEB* in: a) 1987/1988 and c) 1997/1998. Prediction of the modeled round sardinella biomass anomaly (from El Niño 3 SSTs in the previous September) in: b) 1987/1988 and d) 1997/1998. Units in tons/m². In the bottom panel the time evolution of the round sardinella biomass in March off Cape Blanc from *Evol-DEB* (red line) and its prediction from El Niño 3 SSTs in the previous September (blue line).

1
2
3
4
5
6
7
8
9
10 499 over time along the winter months and 2) the dynamical feature of round
11 500 sardinella off northwest Africa is completely different before and after Jan-
12 501 uary, being characterized by a northward migration (searching the Saharan
13 502 bank) in the former case, but by a southward migration, avoiding the cold
14 503 conditions in the Saharan waters from January onwards, in the latter case.
15 504 Accordingly, the specific responses to El Niño identified in the described
16 505 modeling framework and the proposed mechanisms in each sub-season are:

- 19 506 • In early winter (November-January), a weakened northward migration
20 507 of round sardinella. This signal could be explained by an anomalous
21 508 enhancement of the alongshore currents to the south, off the Cape
22 509 Blanc region, due to the El Niño influence.

- 25 510 • In late winter (February-March), an anomalous accumulation of round
26 511 sardinella off Cape Blanc, the underlying mechanism being twofold: 1)
27 512 through a weakening of the alongshore currents to the south (reducing
28 513 the passive advection component of the southward migrations of round
29 514 sardinella) and 2) through an anomalous warming of the surface ocean
30 515 due to a reduction of the coastal upwelling (which improve the habitat
31 516 conditions of round sardinella).

34
35 517 Summarizing, the El Niño-round sardinella teleconnection simulated here
36 518 is mainly explained by the modulating role that the anomalous alongshore
37 519 currents forced by El Niño in the *Cape Blanc Frontal Zone* exerts on the nor-
38 520 mal migration of this species when it avoids water temperatures out of the
39 521 species tolerance and when it follows temperatures close to its natal homing
40 522 conditions. Thus, a general conclusion from the results of this study is that
41 523 a realistic response to El Niño in both, sea temperature and coastal currents,
42 524 is crucial to produce the teleconnection proposed. From a large-scale per-
43 525 spective, there is an extensive literature explaining the dynamical aspects
44 526 associated with the ENSO-TNA teleconnection and it is not a major goal of
45 527 this work to explain this in depth. However, it is worth mentioning how the
46 528 mechanisms presented here are consistent with those accepted by the climate
47 529 community (Enfield and Mayer, 1997, Wang, 2002, 2004, Ham et al., 2014,
48 530 King et al., 2018), reinforcing therefore the robustness of the El Niño-round
49 531 sardinella teleconnection.

52
53
54
55 532
56 533 Although a full validation of the El Niño-round sardinella teleconnection
57 534 is an extremely challenging issue due to the scarcity of reliable data on the

1
2
3
4
5
6
7
8
9
10 535 time varying distribution and abundance fish population, the modeling ap-
11 536 proach presented here seems to be able to simulate a robust ENSO response of
12 537 the environmental conditions off Cape Blanc in winter, closely related to the
13 538 ENSO induced effects in round sardinella biomass (Supplementary material;
14 539 Fig. S5). In this respect, it is worth mentioning that the water tempera-
15 540 ture and ocean current responses described here are consistent with those
16 541 identified in February-March 1998 after the peak of one of the strongest El
17 542 Niño episodes of the last decades (Zeeberg et al., 2008). This reinforces the
18 543 theory of an influence of El Niño on the hydrodynamic conditions along the
19 544 Mauritanian-Saharan coast. This fact, together with the validated skill of
20 545 the modeling strategy used to simulate realistic responses of round sardinella
21 546 to the local environment (Brochier et al., 2018), substantiates the findings of
22 547 this work.
23
24
25
26 548

27 549 In contrast to the major role that food availability plays for determining
28 550 sardine and anchovy abundance in the northern part of the CCUS (Sánchez-
29 551 Garrido et al., 2019), the present analyses indicate that the alteration of the
30 552 variability in nutrient abundance associated with El Niño seems to play a
31 553 minor role for the El Niño-round sardinella teleconnection. This is actually
32 554 consistent with previous works which suggest that the currents and the wa-
33 555 ter temperature are the main environmental variables influencing the round
34 556 sardinella variability in the southern part of this upwelling system (Zeeberg
35 557 et al., 2008, Bacha et al., 2017). However, other studies argue for a weaker
36 558 (Roy and Reason, 2001, Arístegui et al., 2006) or an absent (Cropper et al.,
37 559 2014, Oettli et al., 2016, Gómez-Letona et al., 2017) link between ENSO and
38 560 the northwest African environmental conditions. This apparent inconsistency
39 561 can be explained by diverse causes, such as 1) the distinct manifestations of
40 562 the CCUS variability to the methodology applied (Benazzouz et al., 2014)
41 563 or 2) the fact that in this study, the degrees of freedom of the entire spatio-
42 564 temporal variability of round sardinella were reduced by using the latitude
43 565 as a measure of spatial location (by averaging the biomass in longitude over
44 566 the continental shelf) and by focusing the analysis on a particular mode of
45 567 variability. All this could have contributed to a more efficient identification
46 568 of the El Niño related response in this study.
47
48
49
50
51 569

52
53
54 570 Furthermore, it should not be ruled out that round sardinella could act
55 571 as an ecological integrator of El Niño influence on northwest Africa, show-
56 572 ing even higher correlations than those obtained through the use of other

1
2
3
4
5
6
7
8
9
10 573 environmental fields (e.g., water temperature, currents, or Chl-a), which
11 574 intuitively should be more directly influenced by a remote climate forcing
12 575 (Di Lorenzo and Ohman, 2013). Indeed, the round sardinella mode ana-
13 576 lyzed here presents higher correlations with the Niño index than with the
14 577 local environment (wind stress, meridional current and sea temperature) off
15 578 northwest Africa (Fig. 9). This striking feature had been already found for
16 579 other ecological impacts of ENSO (Capa-Morocho et al., 2014, Diouf et al.,
17 580 2017). The present study suggests a capacity of round sardinella to integrate
18 581 the non-linearities among the climate variables in a unique mode of biomass
19 582 variability.
20
21
22

23 583
24 584 We are aware of the intrinsic limitations of the modeling approach used in
25 585 this study, and we do not expect a perfect match between the real (ideally ob-
26 586 served) and the simulated responses of round sardinella to the environment.
27 587 Nevertheless, this approach provides a highly valuable measure of how the
28 588 spatio-temporal variability of round sardinella reacts to actual climate forc-
29 589 ings (Brochier et al., 2018). Thus, we believe that this study represents a
30 590 valuable step forward in relation to how the global climate can alter local
31 591 responses in marine ecosystems. Furthermore, given that enhanced global re-
32 592 sponses to ENSO are expected under a warmer climate (Frauen et al., 2014),
33 593 the El Niño-round sardinella teleconnection might enhance within the next
34 594 decades. This and other related questions should be further analyzed in fu-
35 595 ture works.
36
37
38
39
40

41 597 **Acknowledgments**

42
43
44 598 The authors thank Davide Zanchettin and Patrice Brehmer for their use-
45 599 ful comments and support during the development of this study. This work
46 600 was funded by the european PREFACE project (No. 603521, Enhancing pre-
47 601 diction of tropical Atlantic climate and its impacts <http://preface.b.uib.no>)
48 602 and by the european TRIATLAS project (No. 817578, South and tropical
49 603 Atlantic climate-based marine ecosystem prediction for sustainable manage-
50 604 ment). Additional support during the writing phase (for P.A. Auger) was
51 605 provided by the Instituto Milenio de Oceanografía (IMO-Chile), funded by
52 606 the Iniciativa Científica Milenio (ICM-Chile).
53
54
55
56
57
58
59
60
61
62
63
64
65

1
2
3
4
5
6
7
8
9 **References**

- 10
11 608 Arístegui, J., Alvarez-Salgado, X. A., Barton, E. D., Figueiras, F. G.,
12 609 Hernandez-Leon, S., Roy, C., Santos, A., 2006. Oceanography and fish-
13 610 eries of the canary current/iberian region of the eastern north atlantic
14 611 (18a, e). The global coastal ocean: Interdisciplinary regional studies and
15 612 syntheses 14, 879.
- 16
17
18 613 Auger, P.-A., Gorgues, T., Machu, E., Aumont, O., Brehmer, P., Nov. 2016.
19 614 [DATASET] What drives the spatial variability of primary productivity
20 615 and matter fluxes in the north-west African upwelling system? A modelling
21 616 approach. Biogeosciences 13, 6419–6440.
- 22
23
24 617 Auger, P. A., Machu, E., Gorgues, T., Grima, N., Waeles, M., 2015. Compar-
25 618 ative study of potential transfer of natural and anthropogenic cadmium to
26 619 plankton communities in the north-west african upwelling. Science of the
27 620 Total Environment 505, 870–888.
- 28
29
30 621 Aumont, O., Bopp, L., Jun. 2006. Globalizing results from ocean in situ iron
31 622 fertilization studies. Global Biogeochemical Cycles 20, GB2017.
- 32
33
34 623 Aumont, O., Maier-Reimer, E., Blain, S., Monfray, P., Jun. 2003. An ecosys-
35 624 tem model of the global ocean including Fe, Si, P colimitations. Global
36 625 Biogeochemical Cycles 17, 29–1.
- 37
38
39 626 Bacha, M., Jeyid, M. A., Vantrepotte, V., Dessailly, D., Amara, R., 2017.
40 627 Environmental effects on the spatio-temporal patterns of abundance and
41 628 distribution of sardina pilchardus and sardinella off the mauritanian coast
42 629 (north-west africa). Fisheries Oceanography 26 (3), 282–298.
- 43
44 630 Báez, J., Santamaría, M., García, A., Gonzalez, J., Hernández, E., Ferri-
45 631 Yáñez, F., 2019. Influence of the arctic oscillations on the sardine off
46 632 northwest africa during the period 1976-1996. VIE ET MILIEU-LIFE AND
47 633 ENVIRONMENT 69 (1), 71–77.
- 48
49
50 634 Bakun, A., 1990. Global climate change and intensification of coastal ocean
51 635 upwelling. Science 247 (4939), 198–201.
- 52
53
54 636 Bakun, A., Black, B. A., Bograd, S. J., Garcia-Reyes, M., Miller, A. J.,
55 637 Rykaczewski, R. R., Sydeman, W. J., 2015. Anticipated effects of climate

- 1
2
3
4
5
6
7
8
9
638 change on coastal upwelling ecosystems. *Current Climate Change Reports*
639 1 (2), 85–93.
- 640 Barton, E., Aristegui, J., Tett, P., Cantón, M., Garcia-Braun, J., Hernández-
641 León, S., Nykjaer, L., Almeida, C., Almunia, J., Ballesteros, S., et al.,
642 1998. The transition zone of the canary current upwelling region. *Progress*
643 *in Oceanography* 41 (4), 455–504.
- 644 Benazzouz, A., Mordane, S., Orbi, A., Chagdali, M., Hilmi, K., Atillah,
645 A., Pelegrí, J. L., Hervé, D., 2014. An improved coastal upwelling index
646 from sea surface temperature using satellite-based approach—the case of the
647 canary current upwelling system. *Continental Shelf Research* 81, 38–54.
- 648 Bez, N., Braham, C.-B., 2014. Indicator variables for a robust estimation of
649 an acoustic index of abundance. *Canadian journal of fisheries and aquatic*
650 *sciences* 71 (5), 709–718.
- 651 Binet, D., 1988. Rôle possible d’une intensification des alizés sur le change-
652 ment de répartition des sardines et sardinelles le long de la côte ouest
653 africaine. *Aquatic living resources* 1 (2), 115–132.
- 654 Boëly, T., Chabanne, J., Fréon, P., Stéquert, B., 1978. Cycle sexuel et migra-
655 tions de sardinella aurita sur le plateau ouest-africain des îles bissagos à la
656 mauritanie. In: *Symp. sur le courant des Canaries: upwelling et ressources*
657 *vivantes. Las Palmas. No. 92. pp. 1–12.*
- 658 Braham, C.-B., Fréon, P., Laurec, A., Demarcq, H., Bez, N., 2014. New
659 insights in the spatial dynamics of sardinella stocks off mauritania (north-
660 west africa) based on logbook data analysis. *Fisheries Research* 154, 195–
661 204.
- 662 Brochier, T., Auger, P.-A., Pecquerie, L., Machu, E., Capet, X., Thiaw, M.,
663 Mbaye, B. C., Braham, C.-B., Ettahiri, O., Charouki, N., et al., 2018.
664 [DATASET] Complex small pelagic fish population patterns arising from
665 individual behavioral responses to their environment. *Progress in Oceanog-*
666 *raphy* 164, 12–27.
- 667 Brochier, T., Echevin, V., Tam, J., Chaigneau, A., Goubanova, K., Bertrand,
668 A., 2013. Climate change scenarios experiments predict a future reduction
669 in small pelagic fish recruitment in the Humboldt current system. *Global*
670 *change biology* 19 (6), 1841–1853.

- 1
2
3
4
5
6
7
8
9
671 Capa-Morocho, M., Rodríguez-Fonseca, B., Ruiz-Ramos, M., 2014. Crop
672 yield as a bioclimatic index of el niño impact in europe: Crop forecast
673 implications. *Agricultural and forest meteorology* 198, 42–52.
- 674 Carr, M.-E., Kearns, E. J., Nov. 2003. Production regimes in four Eastern
675 Boundary Current systems. *Deep Sea Research Part II: Topical Studies in*
676 *Oceanography* 50, 3199–3221.
- 677 Chavez, F. P., Messié, M., 2009. A comparison of eastern boundary upwelling
678 ecosystems. *Progress in Oceanography* 83 (1-4), 80–96.
- 679 Corten, A., Braham, C.-B., Sadegh, A. S., 2017. The development of a fish-
680 meal industry in mauritania and its impact on the regional stocks of sar-
681 dinella and other small pelagics in northwest africa. *Fisheries research* 186,
682 328–336.
- 683 Corten, A., Mendy, A., Diop, H., 2012. La sardinelle de lafrique du nord-
684 ouest: Pêches, évaluation des stocks et la gestion. Sub-Regional Fisheries
685 Commission (SRFC), Dakar.
- 686 Cropper, T. E., Hanna, E., Bigg, G. R., 2014. Spatial and temporal seasonal
687 trends in coastal upwelling off northwest africa, 1981–2012. *Deep Sea Re-*
688 *search Part I: Oceanographic Research Papers* 86, 94–111.
- 689 Czaja, A., van der Vaart, P., Marshall, J., Nov. 2002. A Diagnostic Study
690 of the Role of Remote Forcing in Tropical Atlantic Variability. *Journal of*
691 *Climate* 15, 3280–3290.
- 692 Di Lorenzo, E., Ohman, M. D., 2013. A double-integration hypothesis to
693 explain ocean ecosystem response to climate forcing. *Proceedings of the*
694 *National Academy of Sciences* 110 (7), 2496–2499.
695 URL <http://www.pnas.org/content/110/7/2496>
- 696 Diankha, O., Thiaw, M., Sow, B. A., Brochier, T., GAYE, A. T., Brehmer,
697 P., 2015. Round sardinella (*sardinella aurita*) and anchovy (*engraulis en-*
698 *crasicolus*) abundance as related to temperature in the senegalese waters.
699 *Thalassas* 31 (2), 9–17.
- 700 Diouf, I., Rodriguez-Fonseca, B., Deme, A., Caminade, C., Morse, A. P.,
701 Cisse, M., Sy, I., Dia, I., Ermert, V., Ndione, J.-A., et al., 2017. Com-
702 parison of malaria simulations driven by meteorological observations and

- 1
2
3
4
5
6
7
8
9
703 reanalysis products in senegal. International journal of environmental re-
704 search and public health 14 (10), 1119.
- 705 Ebisuzaki, W., Sep. 1997. A Method to Estimate the Statistical Significance
706 of a Correlation When the Data Are Serially Correlated. Journal of Climate
707 10, 2147–2153.
- 708 Enfield, D. B., Mayer, D. A., Jan. 1997. Tropical Atlantic sea surface tem-
709 perature variability and its relation to El Niño-Southern Oscillation. 102,
710 929–945.
- 711 Failler, P., 2014. Climate variability and food security in africa: the case of
712 small pelagic fish in west africa. Journal of Fisheries & Livestock Produc-
713 tion 2 (2), 1–11.
- 714 Frauen, C., Dommenges, D., Tyrrell, N., Rezný, M., Wales, S., 2014. Analysis
715 of the Nonlinearity of El Niño-Southern Oscillation Teleconnection. 27,
716 6225.
- 717 Fréon, P., Barange, M., Arístegui, J., Dec. 2009. Eastern Boundary Up-
718 welling Ecosystems: Integrative and comparative approaches. Progress in
719 Oceanography 83, 1–14.
- 720 García-Serrano, J., Cassou, C., Douville, H., Giannini, A., Doblado-Reyes,
721 F. J., 2017. Revisiting the enso teleconnection to the tropical north at-
722 lantic. Journal of Climate 30 (17), 6945–6957.
- 723 Giannini, A., Chiang, J. C., Cane, M. A., Kushnir, Y., Seager, R., 2001.
724 The enso teleconnection to the tropical atlantic ocean: Contributions of
725 the remote and local ssts to rainfall variability in the tropical americas.
726 Journal of Climate 14 (24), 4530–4544.
- 727 Gómez-Letona, M., Ramos, A. G., Coca, J., Arístegui, J., 2017. Trends in
728 primary production in the canary current upwelling system: a regional per-
729 spective comparing remote sensing models. Frontiers in Marine Science 4,
730 370.
- 731 Ham, Y.-G., Sung, M.-K., An, S.-I., Schubert, S. D., Kug, J.-S., May 2014.
732 Role of tropical atlantic SST variability as a modulator of El Niño tele-
733 connections. 50, 247–261.

- 1
2
3
4
5
6
7
8
9
734 King, M. P., Herceg-Bulić, I., Bladé, I., García-Serrano, J., Keenlyside, N.,
735 Kucharski, F., Li, C., Sobolowski, S., 2018. Importance of late fall enso
736 teleconnection in the euro-atlantic sector. *Bulletin of the American Mete-*
737 *orological Society* (2018).
- 738 Lee, S.-K., Enfield, D. B., Wang, C., Aug. 2008. Why do some El Niños have
739 no impact on tropical North Atlantic SST? *Geophys. Res. Lett.* 35, 16705.
- 740 Lorenz, E. N., 1956. Empirical orthogonal functions and statistical weather
741 prediction.
- 742 Madec, G., 2008. the nemo team (2008) nemo ocean engine. Note du Pôle de
743 modélisation. Institut Pierre-Simon Laplace (IPSL), France.
- 744 Marchal, E., 1991. Un essai de caractérisation des populations de poissons
745 pélagiques côtiers: cas de sardinella aurita des côtes ouest-africaines.
- 746 Meiners, C., Fernández, L., Salmerón, F., Ramos, A., 2010. Climate variabil-
747 ity and fisheries of black hakes (*merluccius polli* and *merluccius senegalen-*
748 *sis*) in nw africa: A first approach. *Journal of Marine Systems* 80 (3-4),
749 243–247.
- 750 Messié, M., Chavez, F. P., 2015. Seasonal regulation of primary production in
751 eastern boundary upwelling systems. *Progress in Oceanography* 134, 1–18.
- 752 Narayan, N., Paul, A., Mulitza, S., Schulz, M., 2010. Trends in coastal up-
753 welling intensity during the late 20th century. *Ocean Science* 6 (3), 815.
- 754 Oettli, P., Morioka, Y., Yamagata, T., Jan. 2016. A Regional Climate Mode
755 Discovered in the North Atlantic: Dakar Niño/Niña. *Scientific Reports* 6,
756 18782.
- 757 Overland, J. E., Alheit, J., Bakun, A., Hurrell, J. W., Mackas, D. L., Miller,
758 A. J., 2010. Climate controls on marine ecosystems and fish populations.
759 *Journal of Marine Systems* 79 (3-4), 305–315.
- 760 Pauly, D., Christensen, V., Mar. 1995. Primary production required to sus-
761 tain global fisheries. 374, 255–257.
- 762 Polo, I., De Fonseca, B. R., Sheinbaum, J., 2005. Northwest africa upwelling
763 and the atlantic climate variability. *Geophysical research letters* 32 (23).

- 1
2
3
4
5
6
7
8
9
10 764 Rayner, N. A., Parker, D. E., Horton, E. B., Folland, C. K., Alexander,
11 765 L. V., Rowell, D. P., Kent, E. C., Kaplan, A., Jul. 2003. [DATASET]
12 766 Global analyses of sea surface temperature, sea ice, and night marine air
13 767 temperature since the late nineteenth century. 108, 4407.
- 14
15 768 Roy, C., Reason, C., 2001. ENSO related modulation of coastal upwelling in
16 769 the eastern Atlantic. *Progress in Oceanography* 49, 245–255.
- 17
18
19 770 Saha, S., Moorthi, S., Pan, H.-L., Wu, X., Wang, J., Nadiga, S., Tripp, P.,
20 771 Kistler, R., Woollen, J., Behringer, D., Liu, H., Stokes, D., Grumbine, R.,
21 772 Gayno, G., Wang, J., Hou, Y.-T., Chuang, H.-Y., Juang, H.-M. H., Sela,
22 773 J., Iredell, M., Treadon, R., Kleist, D., van Delst, P., Keyser, D., Derber,
23 774 J., Ek, M., Meng, J., Wei, H., Yang, R., Lord, S., van den Dool, H., Kumar,
24 775 A., Wang, W., Long, C., Chelliah, M., Xue, Y., Huang, B., Schemm, J.-K.,
25 776 Ebisuzaki, W., Lin, R., Xie, P., Chen, M., Zhou, S., Higgins, W., Zou, C.-
26 777 Z., Liu, Q., Chen, Y., Han, Y., Cucurull, L., Reynolds, R. W., Rutledge,
27 778 G., Goldberg, M., Aug. 2010. [DATASET] The NCEP Climate Forecast
28 779 System Reanalysis. *Bulletin of the American Meteorological Society* 91,
29 780 1015–1057.
- 30
31
32
33
34 781 Sánchez-Garrido, J., Werner, F., Fiechter, J., Rose, K., Curchitser, E.,
35 782 Ramos, A., Lafuente, J. G., Arístegui, J., Hernández-León, S., San-
36 783 tana, A. R., 2019. Decadal-scale variability of sardine and anchovy simu-
37 784 lated with an end-to-end coupled model of the canary current ecosystem.
38 785 *Progress in Oceanography* 171, 212–230.
- 39
40
41 786 Shchepetkin, A. F., McWilliams, J. C., 2005. The regional oceanic model-
42 787 ing system (ROMS): a split-explicit, free-surface, topography-following-
43 788 coordinate oceanic model. *Ocean Modelling* 9, 347–404.
- 44
45
46 789 Taschetto, A., Rodrigues, R., Meehl, G., McGregor, S., England, M., 2016.
47 790 How sensitive are the pacific–tropical north atlantic teleconnections to the
48 791 position and intensity of el niño-related warming? *Climate dynamics* 46 (5-
49 792 6), 1841–1860.
- 50
51 793 Tsikliras, A. C., Antonopoulou, E., 2006. Reproductive biology of round sar-
52 794 dinella (*sardinella aurita*) in north-eastern mediterranean. *Scientia Marina*
53 795 70 (2), 281–290.
- 54
55
56
57
58
59
60
61
62
63
64
65

1
2
3
4
5
6
7
8
9
10
11
12
13
14
15
16
17
18
19
20
21
22
23
24
25
26
27
28
29
30
31
32
33
34
35
36
37
38
39
40
41
42
43
44
45
46
47
48
49
50
51
52
53
54
55
56
57
58
59
60
61
62
63
64
65

796 Visbeck, M., Chassignet, E. P., Curry, R. G., Delworth, T. L., Dickson, R. R.,
797 Krahmann, G., 2003. The ocean's response to North Atlantic Oscillation
798 variability. AGU Geophysical Monograph Series 134, 113–145.

799 Wang, C., Feb. 2002. Atmospheric Circulation Cells Associated with the El
800 Niño-Southern Oscillation. 15, 399–419.

801 Wang, C., 2004. ENSO, Atlantic climate variability, and the Walker and
802 Hadley circulations. In: The Hadley circulation: Present, past and future.
803 Springer, pp. 173–202.

804 Wilks, D. S., 2011. Statistical methods in the atmospheric sciences. Vol. 100.
805 Academic press.

806 Wooster, W. S., Bakun, A., McLain, D. R., 1976. Seasonal upwelling cy-
807 cle along the eastern boundary of the north atlantic. Journal of Marine
808 Research 34 (2), 131–141.

809 Zeeberg, J., Corten, A., Tjoe-Awie, P., Coca, J., Hamady, B., 2008. Climate
810 modulates the effects of sardinella aurita fisheries off northwest africa. Fish-
811 eries Research 89 (1), 65–75.

1
2
3
4
5
6
7
8
9
10
11
12
13
14
15
16
17
18
19
20
21
22
23
24
25
26
27
28
29
30
31
32
33
34
35
36
37
38
39
40
41
42
43
44
45
46
47
48
49
50
51
52
53
54
55
56
57
58
59
60
61
62
63
64
65

Supplementary material of the manuscript
entitled “El Niño as a predictor of round
sardinella distribution along the northwest
African coast”

April 1, 2020

1
2
3
4
5
6
7
8
9
10
11
12
13
14
15
16
17
18
19
20
21
22
23
24
25
26
27
28
29
30
31
32
33
34
35
36
37
38
39
40
41
42
43
44
45
46
47
48
49
50
51
52
53
54
55
56
57
58
59
60
61
62
63
64
65

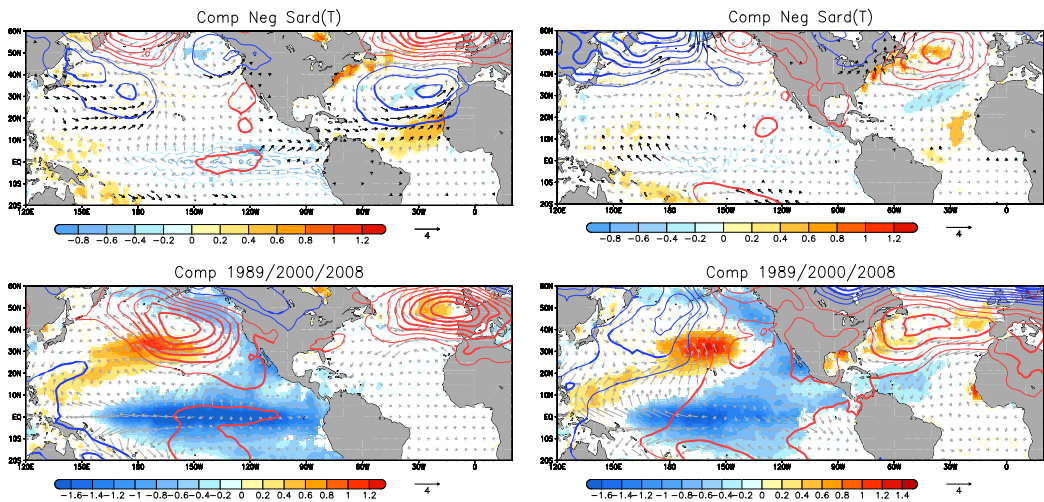


Figure S1: Upper panels: Negative composite maps based on the standardized PC1 (years below -1 standard deviation) of the anomalous round sardinella leading mode. The fields plotted are anomalous SST (shaded the 95% significant response; units in degrees), anomalous SLP (contoured; thick contoured the 95% significant response), and anomalous surface winds (gray vectors; in black the 95% significant response; units in m/s). Bottom panels: the same fields are plotted for La Niña years (years with the Niño 3.4 index below -1 standard deviation). Left panels refer to early winter (Nov-Jan) and right panels to late winter (Feb-Mar).

1
2
3
4
5
6
7
8
9
10
11
12
13
14
15
16
17
18
19
20
21
22
23
24
25
26
27
28
29
30
31
32
33
34
35
36
37
38
39
40
41
42
43
44
45
46
47
48
49
50
51
52
53
54
55
56
57
58
59
60
61
62
63
64
65

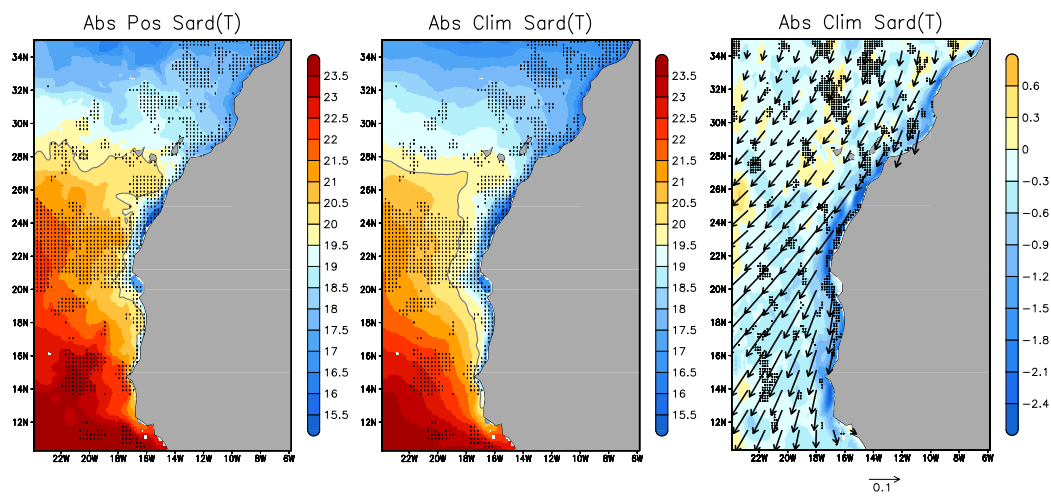


Figure S2: Absolute fields in late winter (Feb-Mar). Temperature of the water column's upper 50 meters under El Niño (left panel) and normal (center panel) conditions. Units in $^{\circ}\text{C}$. Black dots represent areas with significant anomalies in Figure 8c). The 20°C isotherm is contoured for a better interpretation. Right panel represents, under normal conditions, the meridional current averaged in the water column's upper 50 meters (shaded; units in $10 \times \text{m/s}$) and the wind stress (vector; units in N/m^2). Black dots highlight areas with positive significant anomalies in Figure 8d).

1
2
3
4
5
6
7
8
9
10
11
12
13
14
15
16
17
18
19
20
21
22
23
24
25
26
27
28
29
30
31
32
33
34
35
36
37
38
39
40
41
42
43
44
45
46
47
48
49
50
51
52
53
54
55
56
57
58
59
60
61
62
63
64
65

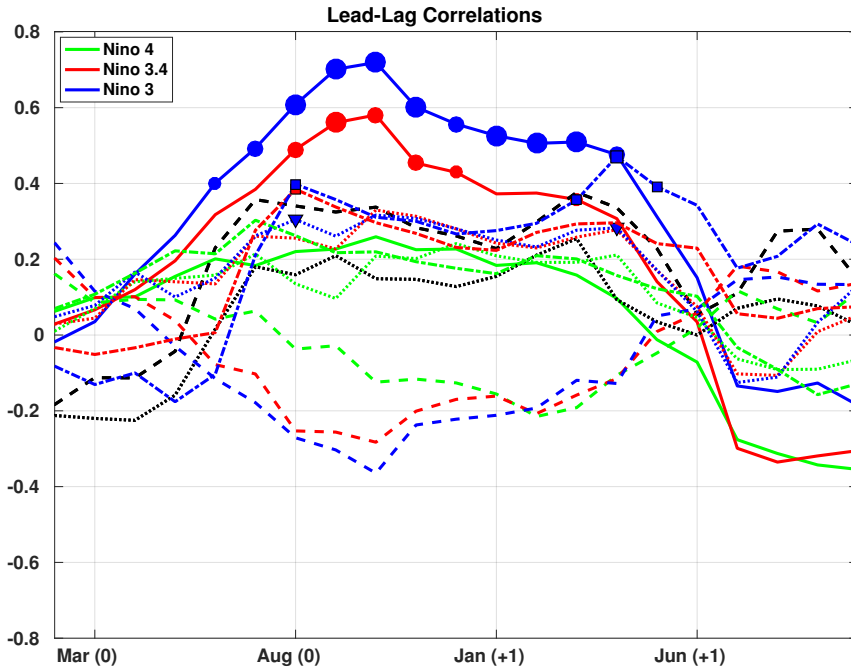


Figure S3: In solid lines the linear correlation coefficients between the leading sardinella mode (i.e., the corresponding PC) in JFM (year +1; see Figure 6a) and the Niño 3 (blue), Niño 4 (green), and Niño 3.4 (red) indices at different time lags. The same is shown for: 1) the meridional current of the water column's upper 50 meters off Cape Blanc in early (dashed lines) and late (dotted lines) winter, and 2) the temperature of the water column's upper 50 meters off Cape Blanc in late winter (dashed-pointed lines). The region off Cape Blanc is defined as the area within the red square indicated in Figure 8. Small, medium and large size of symbols (dots, squares and triangles) represent correlations at the 99%, 95% and 90% confidence level respectively according to the non-parametric test described by Ebisuzaki et al., 2017. Finally, black dashed (dotted) line shows the correlation between the leading sardinella mode and the zonal (meridional) wind stress averaged within the green boxes indicated in Figure 8.

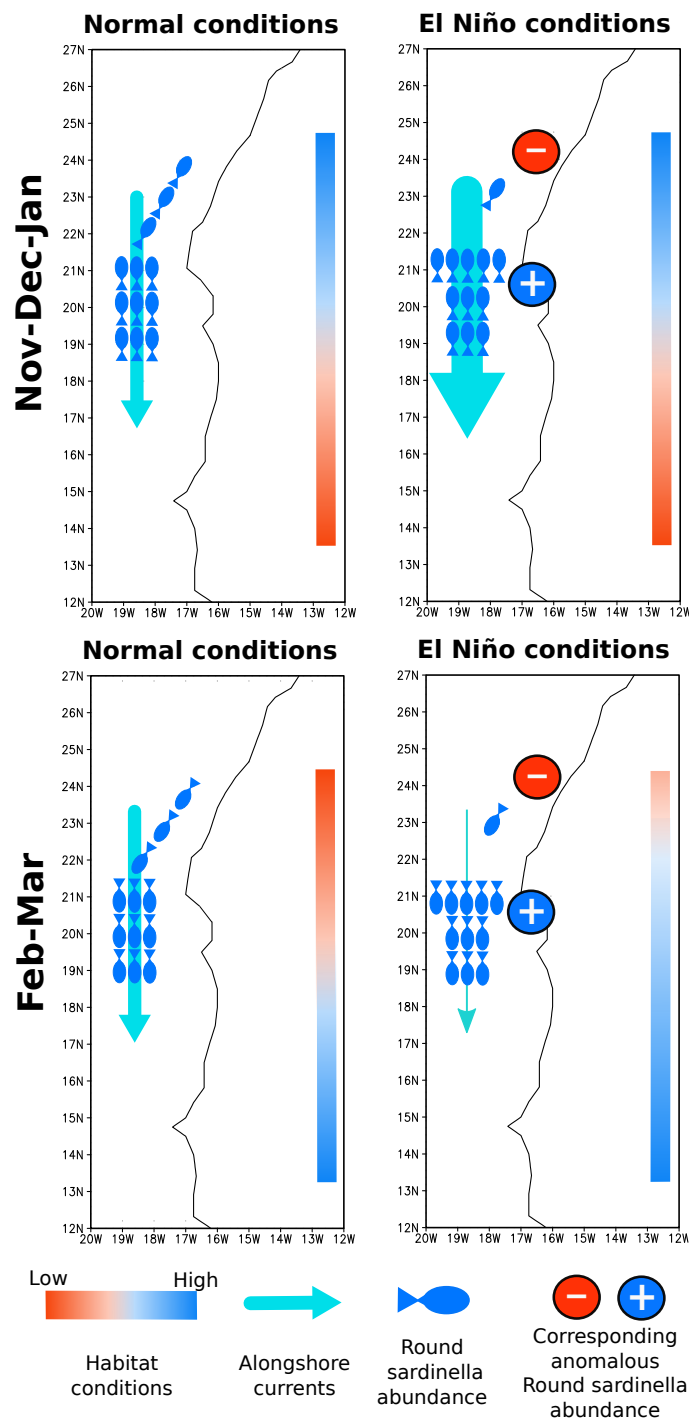


Figure S4: **Simplified representation of the round sardinella response to El Niño.** Upper panels corresponds to early winter and bottom panels to late winter. Left panels correspond to normal conditions and right panels to El Niño influenced conditions. Illustrated the absolute round sardinella biomass, the anomalous biomass response to El Niño, the alongshore currents, and the meridional evolution of the habitat quality of round sardinella (depending on water temperature and food abundance in the water column's upper 50 meters) along the African coast.

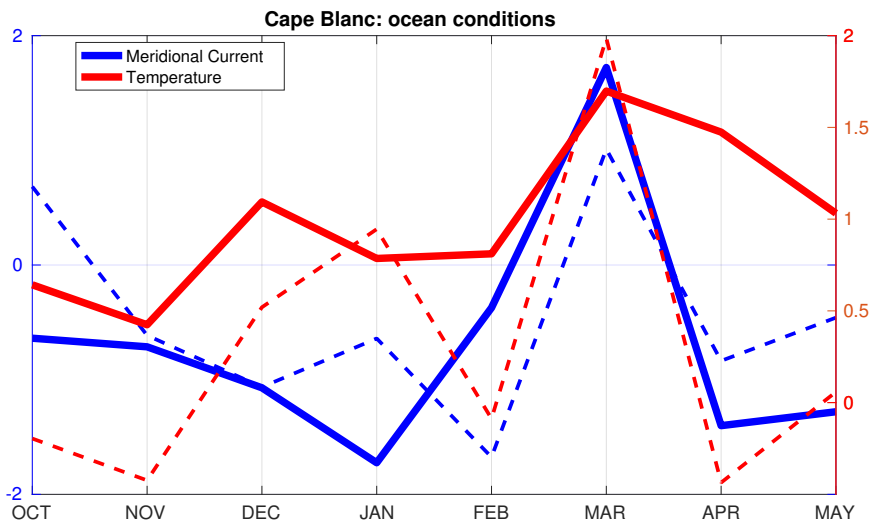


Figure S5: In solid line the averaged evolution, during El Niño years and off Cape Blanc, of the observed sea surface temperature (from the NOAA GHRSSST V.2; https://podaac.jpl.nasa.gov/dataset/AVHRR_OI-NCEI-L4-GLOB-v2.0) and the observed surface meridional current (from OSCAR third degree resolution ocean surface currents; https://podaac.jpl.nasa.gov/dataset/OSCAR_L4_OC_third-deg). In dashed line the same evolution is shown for the modeled (ROMS-PISCES) water temperature and meridional current averaged in the water column's upper 50 meters off Cape Blanc. In all cases the standardized monthly means are calculated in the area within the red square indicated in Figure 8.

Declaration of interests

The authors declare that they have no known competing financial interests or personal relationships that could have appeared to influence the work reported in this paper.

The authors declare the following financial interests/personal relationships which may be considered as potential competing interests:

Declarations of interest: none